Additive manufacturing: haute couture for chemical industries

Authors: Carlos A. Grande [1,*], Jean-Luc Dubois [2], Juan C. Piquero Camblor [3], Ørnulv Vistad, Terje Didriksen [1], Richard Blom [1], Aud I. Spjelkavik [1] and Duncan Akporiaye [1]

Affiliations:

[1]SINTEF Materials and Chemistry. Forskningsveien 1, 0373, Oslo. Norway.

[2]Arkema France. 420 Rue d'Estienne d'Orves, 92705 Colombes. France.

[3]Fundación PRODINTEC. Parque Científico Tecnológico de Gijón. Avda. Jardín Botánico, 1345, 33203 Gijón. Spain.

*Correspondence to: carlos.grande@sintef.no.

Abstract: The energy efficiency and performance of any process run by any chemical company is given by its design. Over the last century, the geometries of the reactors have been changed from ingenious and generally complex configurations to microreactors, aiming to improve mass, energy and momentum transfer. As the complexity of the reactor increases, the limits of manufacturing methods might make the project not viable. These problems will be phased out with the advent of additive manufacturing on a large scale. Additive manufacturing offers the possibility of achieving a tailor-made design of a reactor or separator for a given and specific purpose, opening the doors for a completely new era in reaction and separation engineering. In this communication we will provide some examples that demonstrate the potential of this technique to shift the paradigm of chemical reactors manufacturing.

One Sentence Summary: Additive manufacturing will bring a revolution in reaction and separation engineering by offering tailor-made design of processes for each application.

Main Text: More than 90% of everyday products start their life in chemical plants, either undergoing chemical transformations in reactors or being purified in various stages of separation. Even though the role of chemical reactions dates back to more than five hundred years with the alchemists, the industrial apparatuses used for most of the transformations are still rather standardized. For example, how many continuous flow reactors are not in the form of a cylindrical vessel? There are some exceptions, but their number is limited mostly due to cost of manufacturing complex configurations. If specific reactions are limited by different factors (mass transfer, mixing, thermal management) then their reactors should be customized to give maximum performance. However, the state-of-the-art is that the reactions are fitted into a limited selection of existing designs. Using the example of clothing, it is as if all reactions have to wear a shirt and a pair of jeans. Different sizes are available and some "color" combinations are possible, but most reactors follow the "prêt-à-porter" concept. So if you do not feel comfortable with certain combination of clothes, the same is also true for reactions. Their "poor fitting" is reflected in reduced performance associated with high energy consumption or operations that are resource-intensive.

Initial steps towards "customization" of reactors started with the development of micro reactors having tailor-made channel shapes [1-6]. These reactors operate in two dimensions and the small size of the channels allows rapid heat exchange and reduced mass transfer problems.

Unfortunately, the small channels produce a relatively high pressure drop and the laminar flow is not efficient to promote mixing in the channels. The concept is nice, but scaling micro reactors to produce large amounts of chemicals has been challenging, expensive and in some cases, resource intensive. Most of the cost problems are particularly related to the complex steps in reactor manufacturing. To solve cost issues and mass transfer, an option is to move away from the micrometer size to the millimeter size, with larger channels and as much elements as necessary to improve mixing. In larger scale industrial applications, customization is not common because of costs issues related to manufacture. So at present, these processes are operating at an optimized energy efficiency, but sometimes, this can be far from "the best achievable".

The concept of additive manufacturing (more popularly known as 3D printing) can change forever the manufacture of reactors and other units in chemical plants [7-9]. The driving force for its implementation is that it can be used for extensive improvement in reactions and separations that are strongly limited by mass, momentum or energy transfer in current unitary processes. In that sense and again, using the analogy of clothing, additive manufacturing is the "haute-couture" alternative for reactions and separations allowing customized outfits. However, additive manufacturing can also provide haute couture components (catalysts, internal mixers, etc.) for sensitive processes involving costly chemicals. The new generation of custom-made types of reactors can have a significant impact in terms of energy efficient production of fine chemicals and pharmaceutical products that are currently produced using relatively large batch reactors. Using additive manufacturing, process intensification can be taken to the next level [10-12].

In generic terms, consider the conservation equations of mass, momentum and energy transfer applied for a given process as shown in Table 1. Using additive manufacturing it is possible to modify and "play" individually with every single term in all these equations, introducing design modifications that will potentially improve all transfer problems independently. For catalytic reactors and some separations, the modifications can go down to the level of the structure of the material, whereby detailed control of the porosity can now be achieved. It can furthermore help in significantly reducing the cost of manufacturing and integrating micro reactors with existing plants. One of the major improvements is that all these advantages are achieved using less resources than with conventional manufacturing techniques and in some cases, less energy also [13-15]. Examples will be presented to show the potential of additive manufacturing in contributing with advanced processes and materials to contribute to higher efficiency of chemical industries.

Table 1. Mass, momentum and energy conservation equations for most single-phase reactors and separators.

Mass	$\frac{\partial C_i}{\partial t} + \boldsymbol{u} \cdot \nabla C_i = \nabla \cdot (D \nabla C_i) + R_i$
Momentum	$\rho \frac{\partial \boldsymbol{u}}{\partial t} + \rho(\boldsymbol{u} \cdot \nabla)\boldsymbol{u} = \nabla \cdot \left[-p\boldsymbol{I} + \mu(\nabla \boldsymbol{u} + (\nabla \boldsymbol{u})^T) - \frac{2}{3}\mu(\nabla \cdot \boldsymbol{u})\boldsymbol{I} \right] + \boldsymbol{F}$
Energy	$\rho C_p \frac{\partial T}{\partial t} + \rho C_p \boldsymbol{u} \cdot \nabla T = \nabla \cdot (\lambda \nabla T) + Q$

Structured materials.

Developments in 3D printing of ceramic materials (alumina and other oxides) and metals have been continuously increasing and now it is possible to achieve a very good accuracy with a very wide range of materials. Utilization of structured materials (catalysts, adsorbers, etc.) and structured packing have been increasing, with honeycomb monoliths being good examples. A very important reason for monolith market growth is the very low pressure drop when compared to packed beds, which can achieve pressure drops 70 times lower [16]. Unfortunately, the energy and mass transfer inside each channel are entirely dominated by molecular diffusion or by film mass transfer (for thermal and/or mass transfer) [17, 18]. So if the channels of the honeycomb are "large" to reduce the overall pressure drop, the molecules in the center of the channel have difficulties diffusing to the surface where reaction or adsorption takes place. The problem is commonly solved by increasing the length of the honeycomb, but this means occupying more space and loading more precious metals, as for the case of catalytic converters in cars.

Using additive manufacturing for fabrication of the honeycomb, the shape of the channel can be precisely tailored for the mixture to be treated achieving advantages of having full control and variation of shape and size along the entire length axis, something that cannot be done by extrusion. Two possible modifications to honeycombs are shown in Figure 1: introducing elements for disrupting flow-patterns or making asymmetric channels (or combinations of them). In both cases, changing the laminar profile inside the channel results in better mass transfer.

Catalytic reactors.

Catalytic reactors and separation processes can benefit enormously from innovative designs. Challenges that have to be addressed in the designs are mixing of fluid phase and catalyst / separating agents, energy transfer from strongly exothermic or endothermic reactions, among others.

Static mixers have been a sound concept that have found applications in different fields due to the improved performance given by tailored design. Among the innovative reactors the Netmix concept is an example of optimized mixing [19, 20]. In this technology, a series of tanks is interconnected by transport tubes forming a network of "perfectly" stirred tanks. In this technology, the degree of separation of the inlet tubing is very important to define the quality of mixing. The best mixing should be obtained with a separation of 180 º, which results in two impingent streams in each tank. However, this optimum configuration cannot be achieved in the 2D case of Netmix technology. With additive manufacturing, it is possible to fabricate a successive series of impingent reactors with a much better mixing under similar conditions as shown in Figure 2. Moreover, it is possible to optimize the location of the inlets and outlets so that the mixing can be even better. A comparison of different mixing in cylinder, sphere and 3D sphere single tank is shown in Figure 2. Using additive manufacturing for realizing this concept, the reactor can be produced as a single piece, easily solving pressure leaks and the need of complicated connections or assemblies. We have used such a reactor made with three successive tanks to synthesize HKUST-1 metal-organic framework material with a very short residence time. Using this concept it is possible to control the size distribution of the crystals and eventually its morphology, similarly to other flow chemistry techniques used for materials preparation [21, 22]. The small reactor printed in stainless steel could easily withstand a pressure of 80 bar of helium, demonstrating enough integrity to perform other complex reactions.

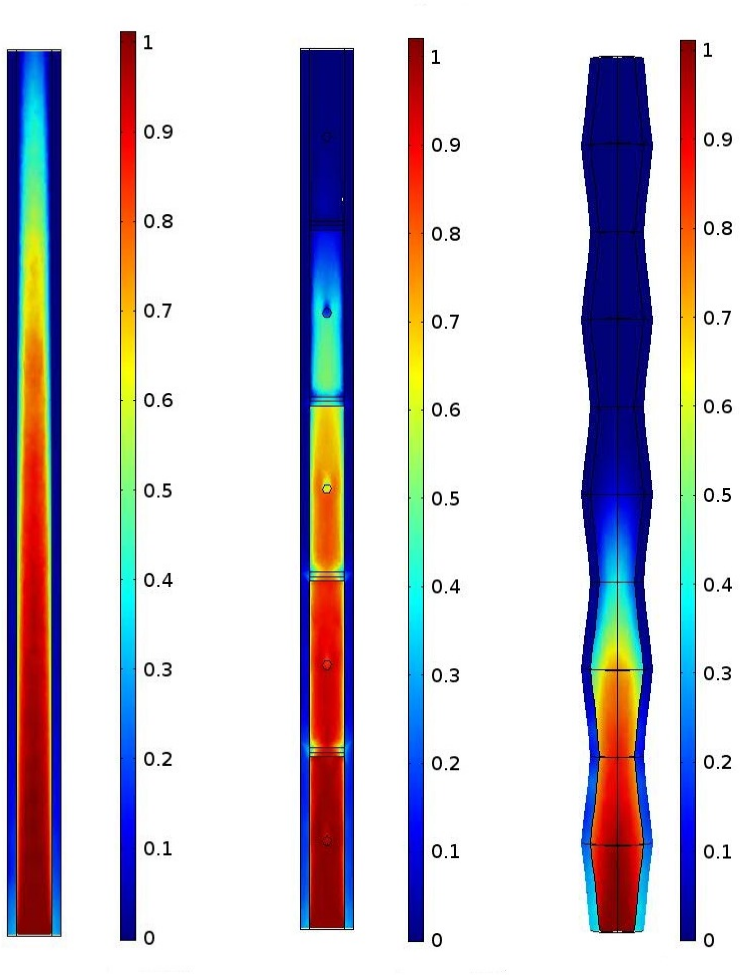

Fig. 1. Different channel geometries for honeycomb monoliths and their flow distribution pattern.

In order to perform fast reactions it is also necessary to have a high degree of micro-mixing in the reactor. When this concept is introduced in reaction engineering books, a generic picture is shown (see Figure 3) [23]. Realizing such configuration in practice was difficult, but using additive manufacturing practical limitations are trivial now. Indeed, the design can be tailor-made so that a better flow distribution can be obtained as shown in Figure 3. Moreover, additive manufacturing offers the possibility to print moving internals so that if the inlets of the reactor are properly tuned, the mixing energy can be provided by the kinetic (or potential) energy of the incoming stream(s).

In this communication we are just introducing and illustrating the potential that additive manufacturing can have for the chemical industry in the coming years. Even more exciting designs in reactor engineering can arise when non-isothermal reactions are considered or for catalysts and reactors dealing with multi-phase mixtures. In such cases and also particularly for the case of very corrosive mixtures, it is even possible to print tailored reactors in titanium, a

feature that has not been possible before. In order to move the technology readiness level (TRL) to commercialization stages, normative for safety, testing and control of the produced reactors should also be put in place.

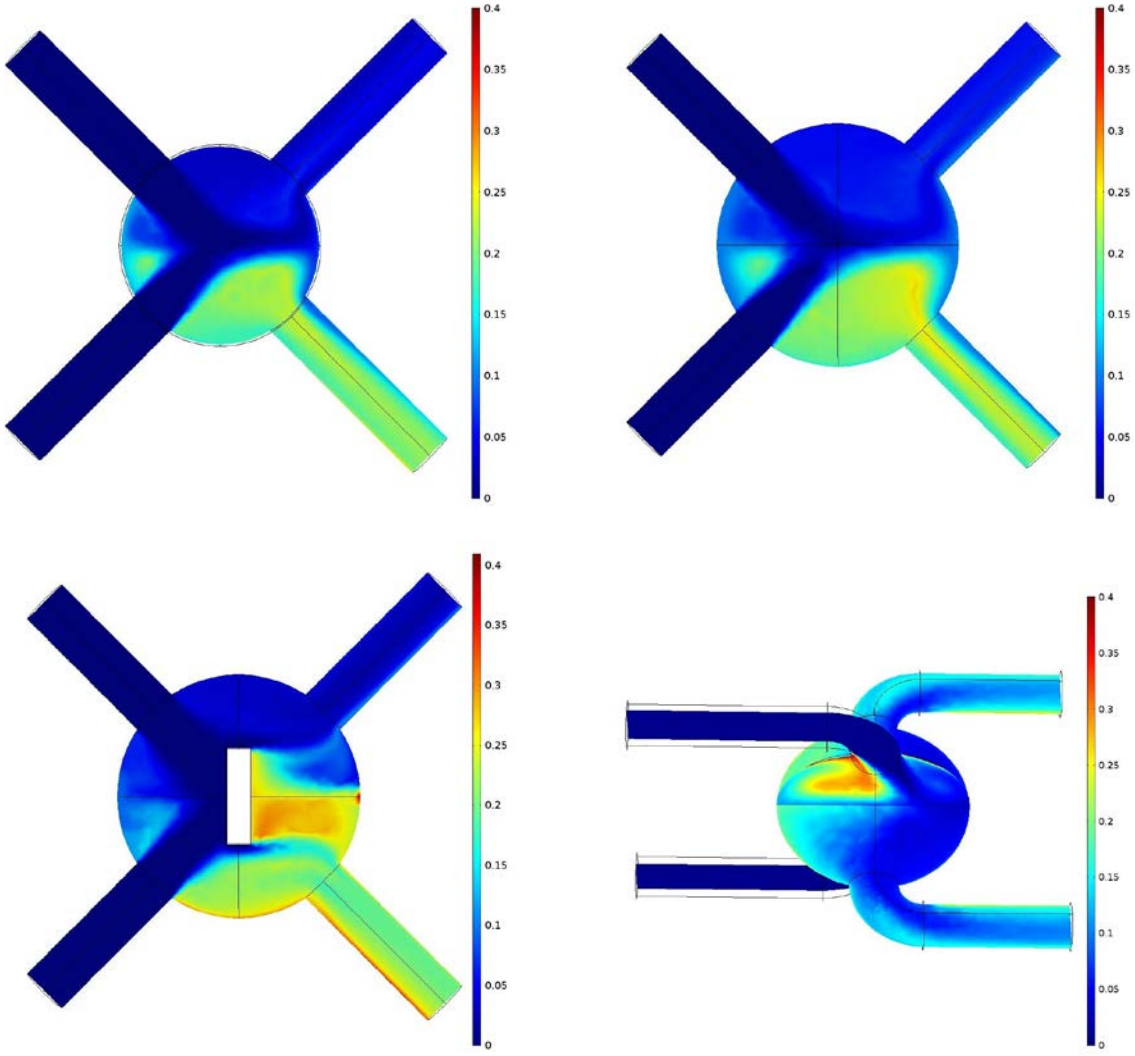

Fig. 2. Distribution of concentration of desired component (two fast reactions in parallel) in unit cells of different static-mixer reactors.

It is true that perhaps producing a piece of catalyst or a reactor with this technology will be expensive but for some applications, the gain in efficiency can compensate the initial investment. With the speed of printers increasing as they are doing now [24], this might not be a significant problem in the near future. Moreover, it is widely known that additive manufacturing is a good tool for prototyping. Considering that large industries only produce a reactor every >20 years, it can be considered as a prototype and it is possible to envision mobile printers installing and manufacturing large reactors onsite, with fewer external limitations (road transport for example) and costs than nowadays.

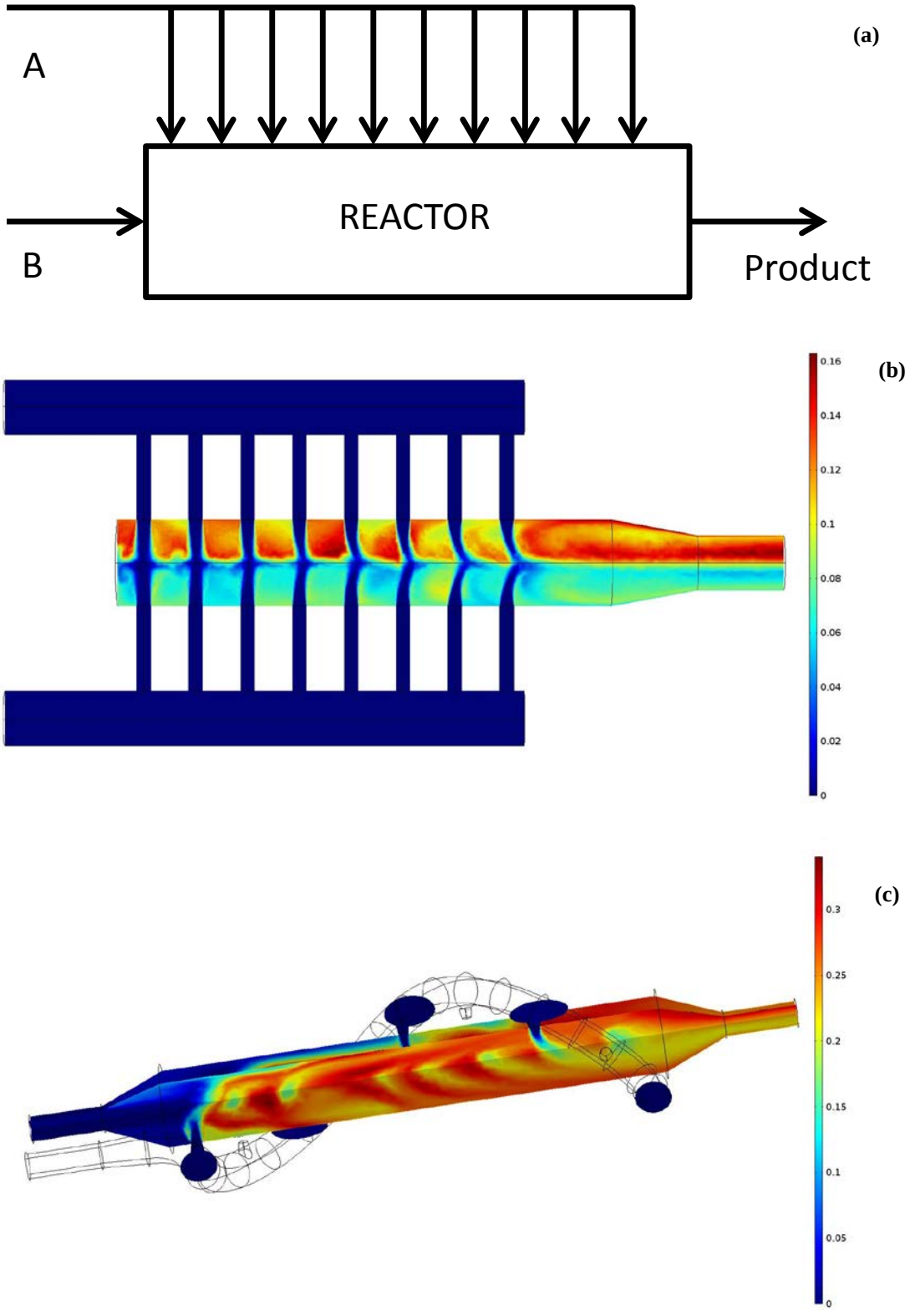

Fig. 3. Ideal distributed flow in continuous reactor (a) [23] and distribution of concentration of desired component (two fast reactions in parallel) in different examples of reactors resembling the continuous multi-feed entrance (b,c).

In terms of development, using additive manufacturing will certainly involve complex computational fluid dynamics (CFD) in an early stage even for the optimization of the design. This is a very important change in the design procedures because it might also require some changes to educational programs to get engineers with the right skills. The new paradigm we envision for the design of optimized reactors in a longer term is shown in Figure 4. Additional advantage is that the prototype, pilot and final reactor can eventually be printed using the same file. This new concept will make companies perform their daily and long term R&D in a different pathway as nowadays, enhancing the need of well-trained engineers, but also of creative minds. Registration of intellectual property and particularly infringements to what is stated in the patents should have to be revised also.

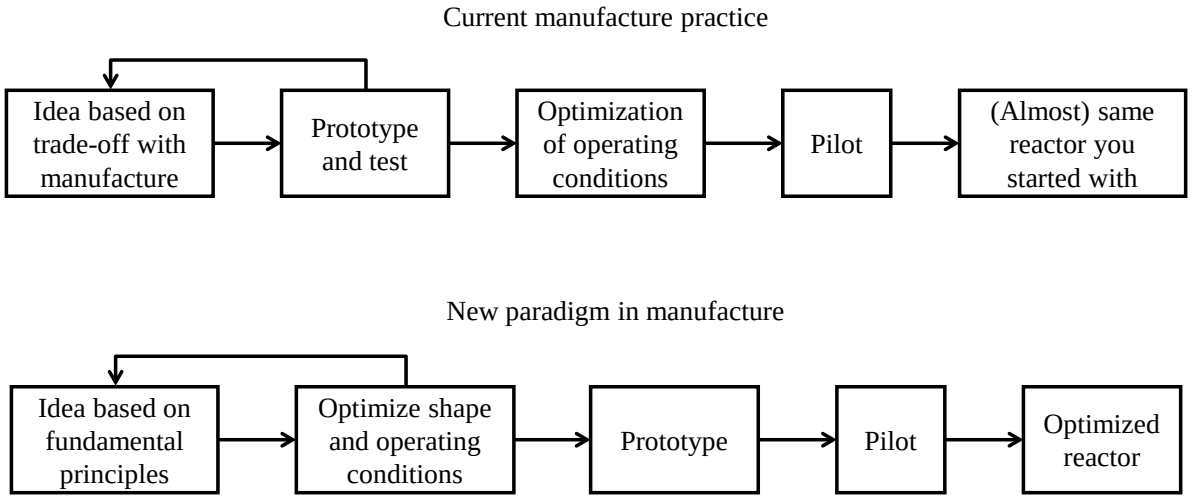

Fig. 4. Current manufacture practice (top) and new paradigm for fabricating optimized reactors using additive manufacturing (bottom).

With all these advantages, we believe that additive manufacturing will emerge as the new-generation toolbox of process intensification, helping chemical industry to improve efficiency and make reactions "move forward" much better. Same as when we have customized clothes.

References:

1. W. Ehrfeld, V. Hessel, H. Löwe. *Microreactors: New Technology for Modern Chemistry*. Wiley-VCH, **2000**.
2. G. M. Whitesides. The origins and the future of microfluidics. *Nature*, 442, 368-373 (2006).
3. P. Kündig. The future of organic synthesis. Science, 314, 430-431 (2006).
4. W. Bier et al., Gas to gas heat transfer in micro heat exchangers. Chem. Engng. Proc., 32, 33-43 (1993).

5. T. M. Squires, S. R. Quake. Microfluidics: Fluid physics at the nanoliter scale. *Rev. Mod. Phys.*, **2005**, 77, 977-1026
6. B. P Mason et al. Greener approaches to organic synthesis using microreactor technology. Chem. Rev., 107, 2300-2318 (2007).
7. The Economist. 3D Printing Scales Up. 7th September 2013
8. K. Kovac. *How Green is 3D Printing?* Ecos Magazine (December 2013).
9. M. D. Symes et al. Integrated 3D-printed reactionware for chemical synthesis and analysis. *Nature Chemistry*, 4, 349-354 (2012).
10. Buchholz, S. *Demonstrating a New Paradigm in Sustainable Manufacturing*. Available at: http://www.f3factory.com/scripts/pages/en/newsevents/F3_Factory_Newsletter_3.pdf
11. A. I. Stankiewicz, J. A. Moulijn. Process intensification: transforming chemical engineering. *Chem. Eng. Prog.*, 22-34 (January 2000).
12. D. Reay, C. Ramshaw, A. Harvey. *Process Intensification*. Butterworth-Heinemann, **2013.**
13. H-S Yoon *et al*. A comparison of energy consumption in bulk forming, substractive, and additive processes: review and case study. Int. J. Prec. Eng. Manuf. Green Technol., 1, 261-276 (2014).
14. R. Huang *et al*. Energy and emissions saving potential of additive manufacturing: the case of lightweight aircraft components. J. Cleaner Production, in press (2015). doi:10.1016/j.jclepro.2015.04.109
15. M. Kreiger, J. M. Pearce. Environmental life cycle analysis of distributed three dimensional printing and conventional manufacturing of polymer products. *ACS Sustainable Chem. Eng.*, 1, 1511-1519 (2013).
16. A. Cybulski, J. A. Moulijn. *Structured Catalysts and Reactors*. CRC Press, **2005.**
17. M. Uberoi, C. J. Pereira. External mass transfer coefficients for monolith catalysts. Ind. Eng. Chem. Res., 35, 113-116 (1996).
18. R. E. Hayes, S. T. Kolaczkowski. Mass and heat transfer effects in catalytic monolith reactors. Chem. Eng. Sci., 49, 3587-3599 (1994).
19. C. M. Fonte et al. The NETmix reactor: Pressure drop measurements and 3D CFD modelling. Chem. Eng. Res. Des., 91, 2250-2258 (2013).
20. V. M. T. M. Silva et al. A novel continuous industrial process for producing hydroxyapatite nanoparticles. J. Disp. Sci. Technol., 29, 542-547 (2008).
21. J. J. Vericella *et al*. Encapsulated liquid sorbents for carbon dioxide capture. Nature Communications, 6, art. 6124 (2015)
22. Rubio-Martinez *et al*. Versatile, high quality and scalable continuous flow production of metal-organic frameworks. Sci. Rep., 4, art. 5443 (2014).
23. O. Levenspiel. Chemical Reaction Engineering, 3rd Edition. Wiley, 1999.
24. J. R. Tumbleston et al., Continuous Liquid Interface Production of 3D Objects. Science, 347, 1349-1352 (2015).

Acknowledgments: Part of the research performed here was supported by the Research Council of Norway through the CLIMIT program by the SINTERCAP project (233818) and with support from the BIGCCS Centre, performed under the Norwegian research program *Centres for Environment-friendly Energy Research (FME)*. The author acknowledge the following partners for their contributions: ConocoPhillips, Gassco, Shell, Statoil, TOTAL, GDF SUEZ and the Research Council of Norway (193816/S60).

Our acknowledgments to all the partners of the about-to start Horizon 2020 PRINTCR3DIT project, for trusting that this methodology can be used in different scales all across different fields of chemistry.

C. Grande also acknowledges the team of Formlabs (USA) by their very efficient assistance and support.

Supplementary information to: Additive manufacturing: haute couture for chemical industries

Authors: Carlos A. Grande [1,*], Jean-Luc Dubois [2], Juan C. Piquero Camblor [3], Ørnulv Vistad, Terje Didriksen [1], Richard Blom [1], Aud I. Spjelkavik [1] and Duncan Akporiaye [1]

Affiliations:

[1]SINTEF Materials and Chemistry. Forskningsveien 1, 0373, Oslo. Norway.

[2]Arkema France. 420 Rue d'Estienne d'Orves, 92705 Colombes. France.

[3]Fundación PRODINTEC. Parque Científico Tecnológico de Gijón. Avda. Jardín Botánico, 1345, 33203 Gijón. Spain.

Materials and Methods:

Mathematical modelling

All the simulations and the drawing of the reactors and honeycomb monoliths used in this study were performed in COMSOL Multiphysics 4.3a. All simulations were assumed to be isothermal and thus the temperature is constant for all times and positions.

The simulations reported in Figure 1 assume incompressible flow behavior of a gas stream (density = 1 kg/m^3 and viscosity = 10^{-5} Pa.s) where the following reaction takes place:

$$A \rightarrow B \qquad r = 0.1C_A$$

The concentration is C_A = 1 mol/m^3, inlet velocity is 0.2 m/s and pressure at the end of the channel is atmospheric (101.325 kPa).

Simulations in Figures 2 and 3 also consider incompressible flow behavior of a liquid stream (density = 1000 kg/m^3 and viscosity = 10^{-3} Pa.s). In these reactors, two reactions take place and the desired product is E:

$$A + B \rightarrow C + D \qquad r = 100C_AC_B$$

$$A + C \rightarrow E + F \qquad r = 15C_AC_C$$

Other variables are: concentration C_A = C_B =1 mol/m^3, inlet velocity is 0.1 m/s and pressure at the end of the channel is atmospheric (101.325 kPa).

Prototyping and metal printing

All the reactors and monoliths produced in this work were initially drawn in COMSOL software and transformed into an stl file that was further used for printing the objects in polymer and metal (steel and titanium alloys).

Stereolithography printer Form +1 from Formlabs was used to produce polymer prototypes of the reactors. Different accuracies were used depending on the dimensions of the reactors to be produced. All pieces were produced using the Clear resin, with curing following the standard recommendations of the manufacturer.

Pictures of the different reactor prototypes used for simulation in Figure 3 are shown in Figure S1. The images were used for modelling and for their production.

Direct metal sintering of powder beds were used to produce the metal reactors [EOS M280]. The reactors were produced in stainless steel and titanium [Stainless steel Ph1 (conforms composition of DIN 1.4540 and UNS S15500) and titanium Ti64 (analogue to ISO 5832-3)].

The produced part was positioned vertically, due to two main reasons: first of all, the definition of critical geometries previously mentioned. It is necessary to obtain the best quality as possible in the internal channel, which features a longitudinal disposition. Thus, building parallel to the z axis is the best option. Second, internal stresses produced by thermal effect during the sintering process, which could lead to partial deformation once it is removed from the building platform. Avoiding the placement of the largest flat surface on the X-Y plane was the best solution to solve this issue.

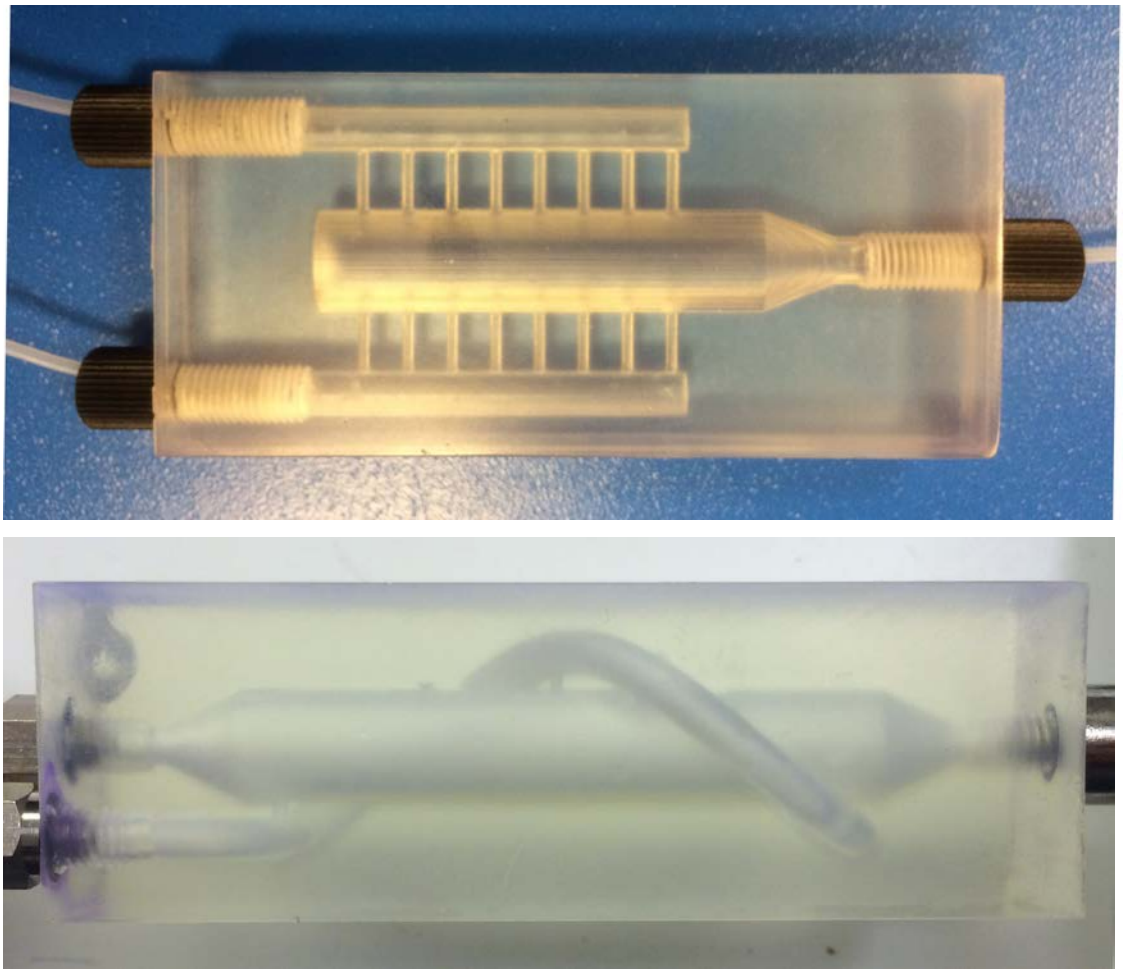

Fig. S1. Examples of reactor prototypes produced by stereolithography that can be directly produced in metal / ceramic.

A comparison of the polymer and metal (without polishing) reactors is shown in Figure S2 together with the image of their topology. For these types of applications where internals are required, the two printers used achieve similar resolutions but with significantly different topologies: the layer-by-layer fabrication of stereolithography and the more random powder bed metal sintering.

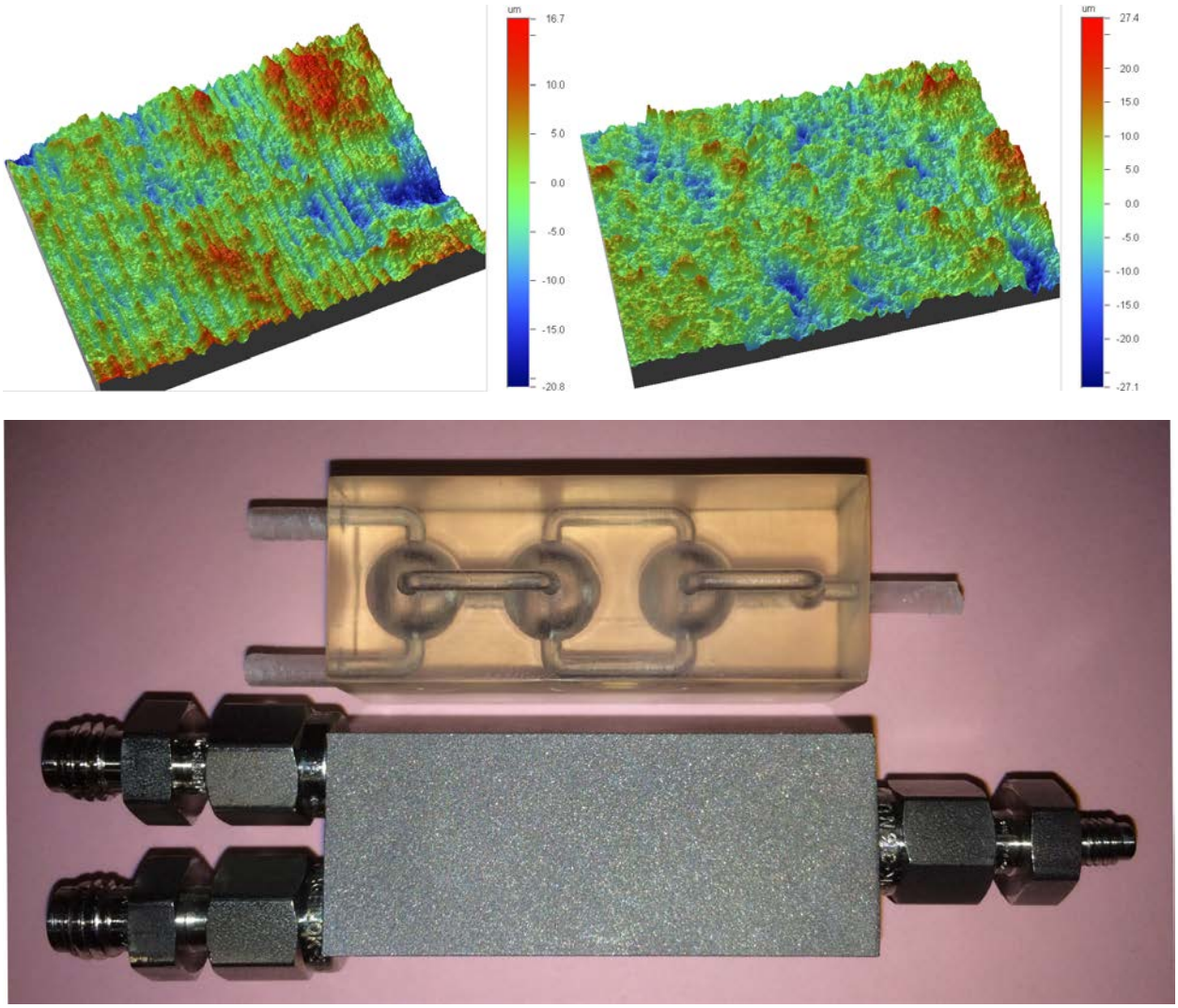

Fig. S2. Prototype and metal reactor used to continuously produce H-KUST-1 metal-organic framework.

Synthesis of HKUST-1

For demonstration purposes, the printed reactor was applied to produce the metal organic framework HKUST-1 in continuous synthesis mode. In typical experiments following known recipes [S1], 6.04 g copper (II) nitrate trihydrate was dissolved in ethanol to produce 250 mL of 0.1M solution, and 12.61 g Benzene-1,3,5-tricarboxylic (BTC) acid was dissolved in ethanol to produce 250 mL of 0.24M solution. The reactor was kept at a temperature of 82 °C. The two solutions were partly preheated and then fed into the reactor by applying a dual head peristaltic pump at a flow rate of 32 mL/min each, resulting in a residence time of 30 s from start to end. Collected materials were filtrated, cleaned by ethanol and dried. Products obtained from the continuous synthesis are compared to a more conventional sample obtained by batch synthesis using the same reactants and reaction temperature. Powder X-ray diffraction(XRD) patterns were recorded on a PANalytical Empyrean diffractometer in reflection mode with Cu K_α radiation (λ=0.15406 nm) operated at 40 kV and 40 mA. The crystalline nature of the HKUST-1 MOF products were confirmed and no impurities detected (Fig S3). The porosity of the samples were examined by N_2 adsorption/desorption measurements performed at 77 K on a Belsorp Mini. The samples were prepared by degassing at 473 K under vacuum for 18 h. Typical type-I isotherms were obtained (Fig 4S) and with BET specific surface area around 1570 m^2/g,

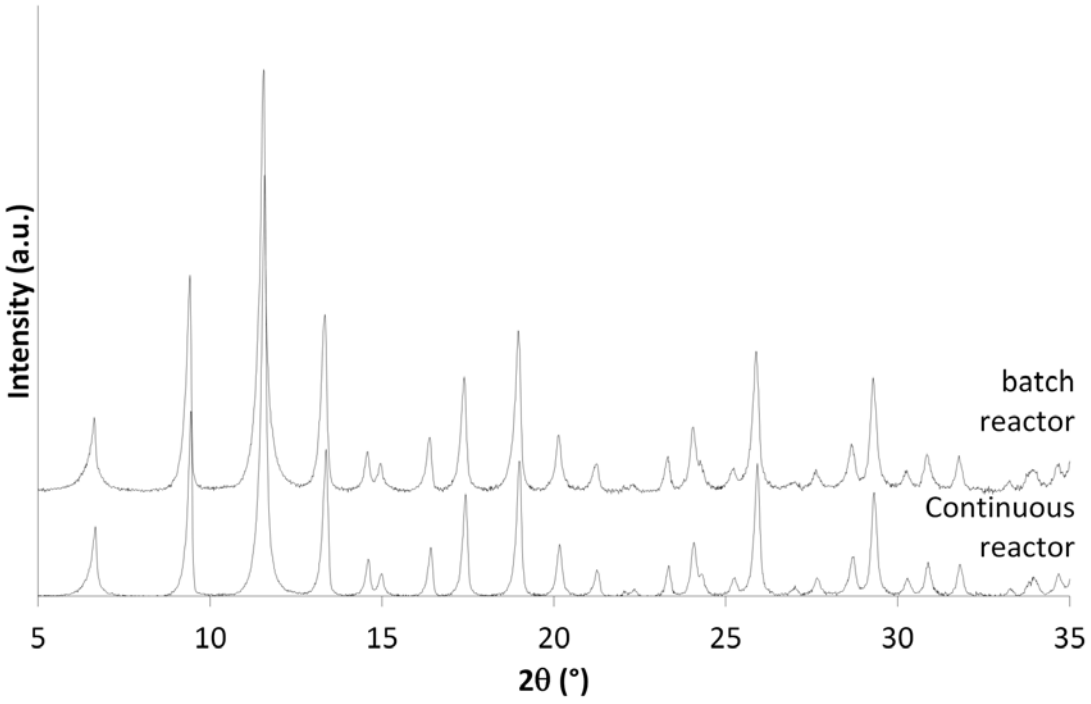

Figure S3. X-ray diffraction patterns showing formation of HKUST-1.

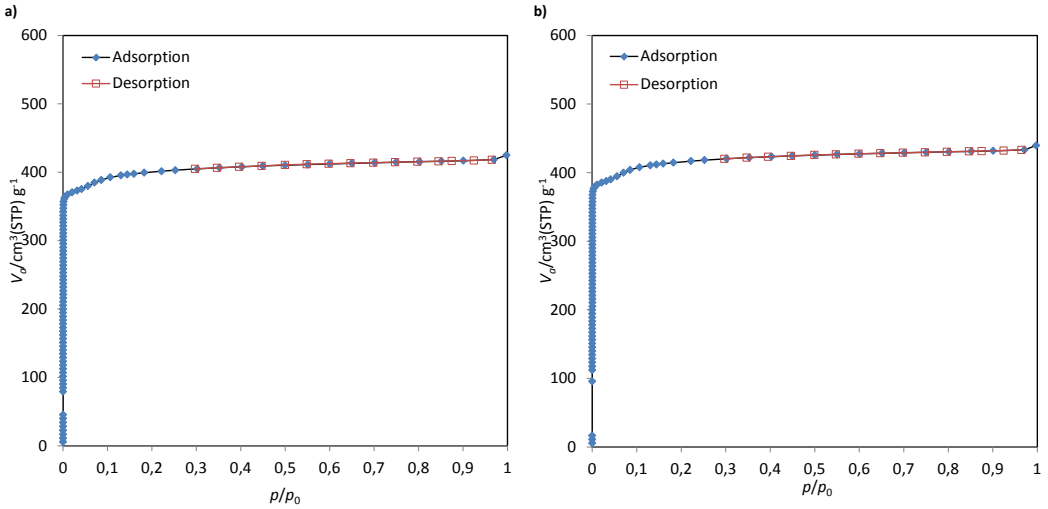

Fig S4. N_2 sorption isotherm for HKUST-1 produced in a) the 3D printed continuous synthesis reactor and b) a batch reactor.

Table S1. Surface area and pore volume of HKUST-1 samples made by 3D printed reactor and by conventional batch synthesis.

	Unit	Continuous reactor	Batch reactor
BET surface	m^2/g	1570	1632
Pore volume	cm^3/g	0.654	0.677
Langmuir surface	m^2/g	1785	1852

Mixing tests in reactors

Macro-mixing tests within the 3D-printed reactor was performed using injections of 10 microliters of methylene blue into one of the inlet ports of the reactor. Different flowrates were used as shown in the results. The exit stream was measured by UV-vis (Shimadzu 1800) with a continuous flow measurement cell of 0.1 microliter to reduce the dead volume at the end of the reactor. The results are shown in Figure S5.

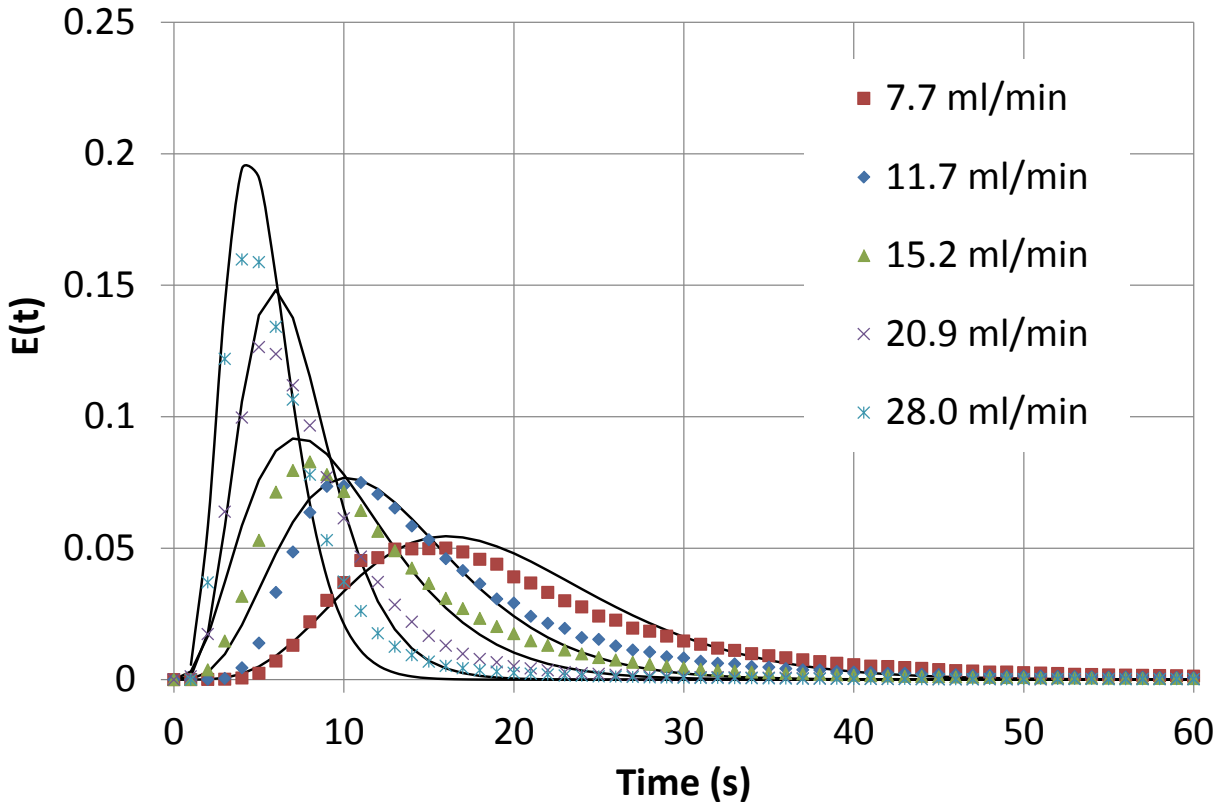

Fig. S5. Distribution of methylene blue at the end of the 3D printed reactor obtained for different inlet flowrates. The solid lines are the fitting of the tank in series model using n=6.

The micro-mixing properties of the mixers were characterized using a modification of the Villermaux/Dushman method [S2]. The method is based on the competing pair of reactions:

$$H_3O^+ + H_2BO_3^- \rightarrow H_2O + H_3BO_3 \quad (extremelly\ fast)$$

$$5I^- + IO_3^- + 6H^+ \rightarrow 3I_2 + 3H_2O \quad (very\ fast)$$

A solution of iodide and iodate in a basic borate buffer (solution A) is mixed with dilute sulfuric acid (solution B). If the mixing is sufficiently good, the acid is neutralized by the buffer before the second reaction occurs, while under conditions of less perfect mixing, the buffer is locally depleted, and the second reaction results in formation of iodine which is then detected spectroscopically. The sensitivity of the test may be tuned by varying the concentrations.

Concentrations employed:

Solution A:

15 mM H_3BO_3, 15 mM NaH_2BO_3, 10 mM KI, and 2 mM KIO_3.

Solution B:

5 mM H_2SO_4

Each of the three mixers was tested using two different flow rates: 7.5 ml/min (total), and 15 ml/min. The solutions were mixed in a 1:1 ratio. After 5 min equilibration time, 100 μl of the reactor effluent was transferred to a BD Flacon Microtest 96-Well 370 μl Plate, and the absorbance was measured at 390 nm^{-1} and at 353 nm^{-1} using a BioTek Power Wave XS plate reading spectrophotometer.

The readings were corrected for the absorbance of an empty well. The results were also compared to the absorbance of a solution obtained by introducing solution A slowly into a stirred quantity of solution B, assuming that maximal iodine concentration would then be obtained. This is numbered as test 1. The tests with the reactor shown in Figure S2 are tests number 2 and 3 while the tests with reactor from Figure S1(a) are number 4 and 5. Finally, the tests with reactor shown in Figure S1(b) correspond to experiments 6 and 7.

Test number	Total flow [ml/min]	Absorbance		Relative to reference	
1-		290 [nm^{-1}]	353 [nm^{-1}]	290 [nm^{-1}]	353 [nm^{-1}]
2- No reactor	-	1.422	0.927	100.0	100.0
3- Figure S2	15.0	0.219	0.135	10.4	6.5
4- Figure S2	7.5	0.351	0.266	20.2	22.0
5- Figure S1(a)	15.0	0.762	0.497	50.8	49.2
6- Figure S1(a)	7.5	0.510	0.331	32.0	29.6
7- Figure S1(b)	15.0	0.548	0.356	34.9	32.6
8- Figure S1(b)	7.5	0.674	0.441	44.3	42.6

References:

S1. M. Rubio-Martinez, *et al*., Versatile, high quality and scalable continuous flow production of metal-organic frameworks. Sci. Rep., 4, art. 5443 (2014).

S2. S. Panic et al., Experimental approaches to a better understanding of mixing performance of microfluidic devices. Chem. Eng. J., 101, 409-419 (2004).